ISBN: 978-3-95450-227-1 ISSN: 2673-5490 doi:10.18429/JACoW-IPAC2022-WEPOMS023

OPTIMIZATION STUDIES OF SIMULATED THz RADIATION AT FLUTE

C. Xu*, E. Bründermann, A. Santamaria Garcia, J. Schäfer, M. Schwarz, A.-S. Müller
Karlsruhe Institute of Technology (KIT), Karlsruhe, Germany

Abstract

The linac-based test facility FLUTE (Ferninfrarot Linac Und Test Experiment) at KIT will be used to study novel accelerator technology and provide intense THz pulses. In this paper, we present start-to-end simulation studies of FLUTE with different bunch charges. We employ a parallel Bayesian optimization algorithm for different bunch charges of FLUTE to find optimized accelerator settings for the generation of intense THz radiation.

INTRODUCTION

The accelerator test facility FLUTE [1] at KIT will be used to generate broadband THz radiation for various experiments. It will operate with a wide range of bunch charges from pC to nC, for which the radiation needs to be optimized. The electron bunch at FLUTE is first created at an RF photoinjector and accelerated up to 7 MeV. It then travels through a linac, which further accelerates the bunch up to 50 MeV. At the end, the bunch is compressed longitudinally via a bunch compressor with 4 dipole magnets down to the fs range, allowing the generation of intense THz pulses with coherent synchrotron radiation (CSR).

Spatial light modulators are being integrated into the photocathode laser system to have 3D control of the laser pulse and provide a tailored initial electron distribution for intense THz pulse generation [2, 3]. In previous studies, a genetic algorithm (GA) was employed in the parameter optimization to minimize the bunch length at 1 pC bunch charge [4]. Nevertheless, it is known that GA is prone to local optima and often requires more computation resources or multiple restarts to mitigate this problem [5]. In this paper, we implement a parallel variant of the Bayesian optimization (BO) [6], which is as efficient as GA and can globally optimize the given physical objective functions even with a large parameter space. We present the first optimization results using parallel Bayesian optimization (PBO) for minimum electron bunch length and maximum peak THz pulse E-field, both for low and high charge cases.

PARALLEL BAYESIAN OPTIMIZATION

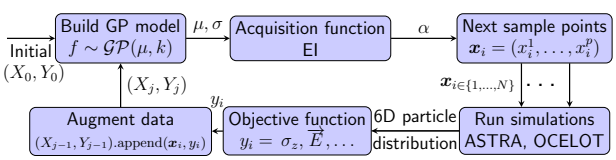

Figure 1: Workflow of the parallel Bayesian optimization algorithm. The boxes are calculations and the arrows are the input and output variables.

* chenran.xu@kit.edu

Bayesian optimization is widely used for global optimization of an unknown objective function $f(x)$. Figure 1 shows the BO algorithm workflow used in this paper. In each step, BO builds a statistical model, where the most widely used is a Gaussian process (GP), of the objective f. The GP model $\mathcal{GP}(\mu, k)$ predicts the mean $\mu(x)$ and uncertainty $\sigma(x)$ of the objective function value $y = f(x)$ at an unknown point $x = (x^1, \ldots, x^p)$, where p is the number of input parameters. The kernel function $k(x, x')$ describes the expected similarity between two data points. In this study, we choose the radial basis function (RBF) as kernel. Based on the GP model, an acquisition function α can be calculated to efficiently guide the optimization and choose the next point to sample x_i. Here we use the expected improvement (EI) [7] acquisition, which calculates the expected value of improvement of a point x over the best observed value so far f_{best}.

In the non-parallel version of BO, the next sample point is selected at the maximum of the acquisition $\alpha_{\text{EI}}(x)$. Since the objective is calculated through physics simulations, we can further increase the performance of BO by evaluating N multiple parameter settings in parallel, with N being the parallel capacity of available computing resources. For the parallel Bayesian optimization (PBO) implementation in this paper, we use a local penalization function to select batch sample points [6]. The i-th sample point x_i is chosen by maximizing the product of acquisition α and penalization function $\varphi_= \varphi_1 * \cdots * \varphi_{i-1}$, where $\varphi_{i-1} \in (0, 1]$ effectively penalizes the acquisition value of a point locally around a previous sample point in the parallel batch x_{i-1}. This allows an efficient sampling of the parameter space in a single optimization step j.

IMPLEMENTATION OF CSR OPTIMIZATION

Based on the knowledge of FLUTE, we choose the following 6 parameter as input for the PBO algorithm: phase and gradient of the photoinjector gun and linac RF field, solenoid magnetic field and the bunch compressor bending angle.

The total spectral intensity of the synchrotron radiation emitted by an electron bunch is

$$\frac{\mathrm{d}^2 I}{\mathrm{d}\omega \mathrm{d}\Omega} = [N_\mathrm{e} + N_\mathrm{e}(N_\mathrm{e} - 1)F(\omega)] \frac{\mathrm{d}^2 I_0}{\mathrm{d}\omega \mathrm{d}\Omega}, \qquad (1)$$

where N_e denotes the number of electrons in the bunch, $F(\omega)$ is the form factor, and $\mathrm{d}^2 I_0/\mathrm{d}\omega\mathrm{d}\Omega$ is the single particle spectral density. The first part is the incoherent radiation, scaling linearly with the electron number N_e. The second part is the coherent synchrotron radiation (CSR), which scales quadratically. Due to the large number of electrons in a bunch, the coherent radiation, where the form factor F is

ISBN: 978-3-95450-227-1 ISSN: 2673-5490 doi:10.18429/JACoW-IPAC2022-WEPOMS023

close to 1, is enhanced by many orders of magnitude. For frequencies corresponding to wavelengths shorter than the bunch length, the form factor F and thus the CSR intensity drop rapidly. We choose the rms bunch length σ_z as an objective function, because minimizing σ_z will extend the form factor $F(\omega)$ to higher frequencies and increase the overall CSR intensity.

Alternatively, we use the peak electric field of the THz pulse as an objective function, which leads to a more direct optimization of the THz pulse despite requiring more processing steps of the output particle distribution. Based on the semi-analytic approach introduced in [8, 9], we are able to calculate the CSR E-field emitted by an arbitrarily shaped bunch

$$\begin{aligned} E(t) &= N_\mathrm{e} \int_{-\infty}^{\infty} E_0(\tau)\varrho(t-\tau)\,\mathrm{d}\tau \\ &= N_\mathrm{e}\frac{1}{\pi}\Re\int_0^{\infty}\tilde{E}_0(\omega)\,\tilde{\varrho}(\omega)\,\mathrm{e}^{\mathrm{i}\omega t}\,\mathrm{d}\omega\,, \end{aligned} \tag{2}$$

where N_e is the number of electrons, E_0 is the single electron E-field, and ϱ is the normalized charge density of the electron bunch. The Fourier-transformed charge density $\tilde{\varrho}(\omega)$ is then obtained analytically via a step-wise linear interpolation of ϱ and the E-field of the bunch emitted CSR in the time-domain, which is numerically integrated for all frequencies.

The complete structure of FLUTE is implemented as a simulation model using the tracking codes ASTRA [10] and OCELOT [11]. The electron bunch is first created by ASTRA and tracked from the cathode to the entrance of the bunch compressor, including the space charge (SC) effect along the track. The ASTRA output particle distribution is then fed into an OCELOT model, which tracks the bunch further until the end of the magnet chicane and, in addition, includes the CSR effects. The final distribution is used to calculate the respective objective function f. For the simulation presented in this paper, 10,000 macro particles were generated and tracked in ASTRA and OCELOT, where each simulation took about 10 min. The parallel Bayesian optimization algorithm was run on a computing cluster with 20 parallel evaluations and a maximum of 50 optimization steps. The optimization took in total about 6 hours, where the majority of time was spent on the time-consuming simulations. For each optimization, we choose the same 20 random sample points to initialize the GP model. The GP hyperparameters, such as the variance and the kernel length scales, are fitted dynamically during the optimizations. Alternatively, these hyperparameters can be estimated from prior knowledge of the physics model or dedicated parameter scan results. Although the later option will require more time, it could further increase the convergence speed of the Bayesian optimization.

RESULTS

We first consider the 1 pC bunch charge case, where the initial distribution is generated by a laser pulse with a transverse size of 0.25 mm and a pulse length of 700 fs. Figure 2(a) shows the longitudinal phase space of the electron bunch using design stage parameter settings obtained from a parameter scan method. The optimization results with bunch length σ_z and peak E-field of the THz pulse E_max as objective are shown in Figs. 2(b) and (c) respectively. The projection onto the time axis corresponds to the current density profile. The bunch length optimization further compresses it down to $\sigma_z = 3.9$ fs. On the other side, the peak E-field optimization manages to keep more electrons in the core of the bunch and reaches a higher peak current, even though with a larger rms bunch length of 4.6 fs.

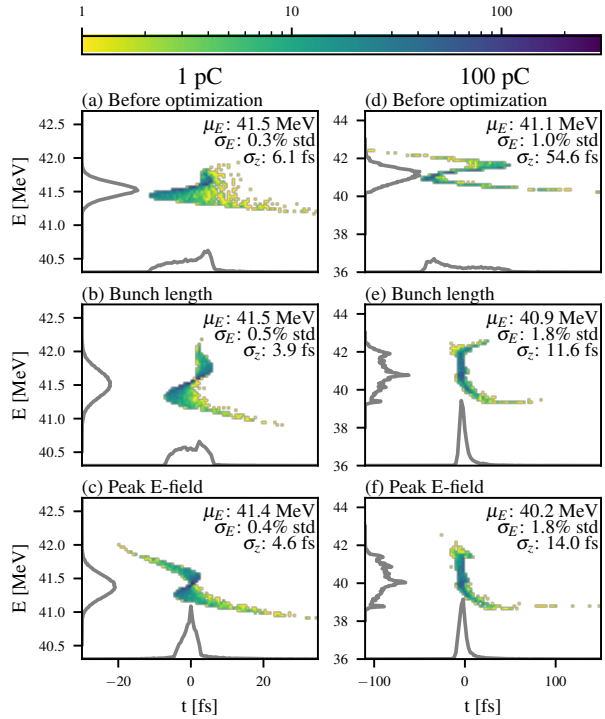

Figure 2: Longitudinal phase space of the compressed electron bunches with (a-c) 1 pC charge and (d-f) 100 pC charge. (a,d) previous settings in design stage, (b,e) optimized settings to minimize bunch length, and (c,f) optimized settings to maximize the peak electric field of THz pulse.

For the high bunch charge case with 100 pC, the initial distribution is generated from a laser pulse with a transverse size of 0.25 mm and a pulse length of 2 ps. Figures 2(d-f) show that the optimizations with both objective functions obtain very similar results and longitudinal phase space distributions. The minimum bunch length $\sigma_z = 11.6$ fs is smaller than the design stage value of 54.6 fs by a factor of ~ 4.7. Both bunches from BO optimizations have an higher energy spread, which is a side effect of moving away from the nominal linac phase for a more linear accelerating gradient and thus a better compression.

The total emitted SR spectrum for different settings are shown in Figs. 3(a,c). It is visible that all the spectra decrease rapidly above the critical frequency $\omega_c \sim 1.4 \times 10^{14}\,\mathrm{s}^{-1}$ (corresponding to ca. 22 THz). For the 1 pC case, the spectrum of the E_max-optimization extends to higher frequencies and has a smooth curve, while the spectra for other settings

ISBN: 978-3-95450-227-1 ISSN: 2673-5490 doi:10.18429/JACoW-IPAC2022-WEPOMS023

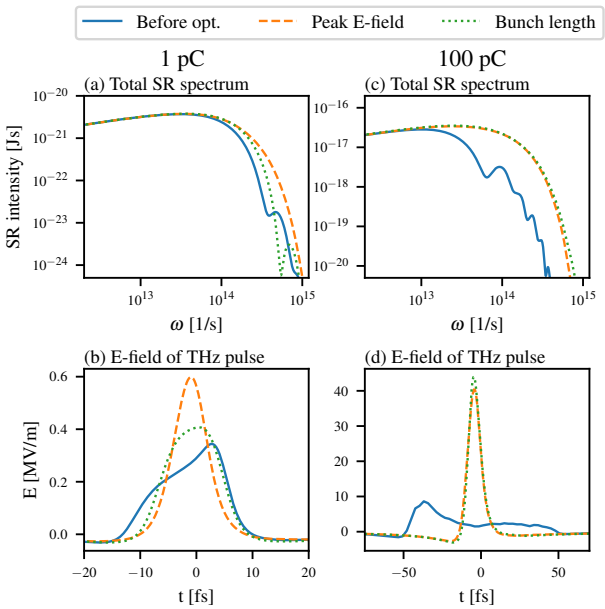

Figure 3: Bunch SR spectrum and THz pulse electric field for (a,b) 1 pC and (c,d) 100 pC bunch charge.

show side bumps in the high-frequency region due to heterogeneous charge densities in the bunch. For each particle distribution, the electric field of the THz pulse is calculated at distance $R = 1$ m and phase $\phi = 0$, as shown in Fig. 3(b,d). For 1 pC bunch charge, the peak E-field of $E_{\max}$-optimization reaches 600 kV/m, which is higher than for the bunch length optimization with 400 kV/m and is higher than the design settings of 350 kV/m by a factor of $\sim$ 1.7. For the design settings, the THz pulse shape follows roughly the shape of the bunch current profile. Decreasing the bunch length further, smoothes the bunch structure. Then, the resulting THz pulse approaches a Gaussian shape with a FWHM of about $1/\omega_c$. Whereas for the 100 pC case, the final bunches are still longer than $1/\omega_c$. Therefore reducing the bunch length efficiently, extends the form factor F to higher frequencies and increases the THz pulse E-field. As shown in Figs. 3(c,d), both settings have a clearly more intense SR. A peak E-field of 43 MV/m is reached, which is higher than the previous design value at 8.4 MV/m by a factor of 5. Due to the inevitably larger bunch length, the THz pulse peak E-field of the 100 pC increases by a factor of $\sim$ 70 compared to the 1 pC case, despite having a 100 times higher bunch charge.

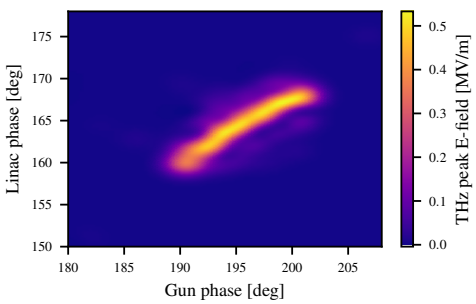

Figure 4: Example of GP predicted parameter space.

The minimal rms bunch length obtained by BO at 1 pC is slightly longer than the previous GA result with $\sigma_z = 3.2$ fs, obtained from a different initial bunch setting. The final THz pulses and optimized accelerator parameters are comparable. This is due to the large parameter space for exploration and a small number of allowed steps. To mitigate this, one can consider running a follow-up BO or a GA optimization with a smaller parameter range around the optimal points. Additionally, BO builds a probabilistic model along the optimization, while GA only keeps a set of best settings in memory. After optimizations, the resulting GP posterior can also be used as a surrogate of the parameter space. For example, Fig. 4 shows the 2D GP posterior subspace of gun and linac RF phases, where a positive linear correlation between the phase settings of gun and linac is clearly visible. This is fully consistent with the physics expectation, as the gun and linac are placed with a fixed distance, which corresponds to a fixed phase advance. Large deviation from it results in unmatched phase and consequently a lower THz pulse intensity.

CONCLUSION AND OUTLOOK

We implemented a parallel version of the Bayesian optimization algorithm, which can be run on a cluster to speed up the parameter optimization. The accelerator settings for FLUTE were optimized for bunch charges of 1 pC as well as 100 pC and for two objectives: minimizing the bunch length and maximizing the CSR THz pulse electric field. The peak E-field proves to be a more suitable objective as it encodes more information about the bunch and leads to a more direct optimization. With the small number of parameters and two individual objectives in this study, the constructed GP model is relatively simple and provides optimized results fast and with good statistics. However, the outcome is more or less predictable. In contrast, in more complex systems, the GP model could help unveiling unknown trends and correlations between machine parameters. BO is a useful tool to quickly optimize the parameter settings during the design phase of a new accelerator or for new operation modes, but one has to carefully design the objective function. It can also help to understand the correlation between the physical parameters with the GP posterior prediction. We plan to implement more coherent synchrotron radiation types as optimization objectives, for example transition radiation and edge radiation. Additionally, parallel BO can be further extended to allow Pareto-front optimization for different objectives, e.g. finding the minimal bunch lengths for electron bunches with highest possible energy.

ACKNOWLEDGEMENTS

This work is in part funded by the Initiative and Networking Fund by the Helmholtz Association (Autonomous Accelerator, ZT-I-PF-5-6). C. Xu and J. Schäfer acknowledge the support by the DFG- funded Doctoral School “Karlsruhe School of Elementary and Astroparticle Physics: Science and Technology”.

ISBN: 978-3-95450-227-1 ISSN: 2673-5490 doi:10.18429/JACoW-IPAC2022-WEPOMS023

REFERENCES

[1] M. J. Nasse *et al.*, "FLUTE: A versatile linac-based THz source," *Review of Scientific Instruments*, vol. 84, no. 2, p. 022 705, 2013, doi:10.1063/1.4790431

[2] C. Xu *et al.*, "Machine Learning Based Spatial Light Modulator Control for the Photoinjector Laser at FLUTE," in *Proc. IPAC'21*, Campinas, Brazil, May 2021, pp. 3332–3335, doi:10.18429/JACoW-IPAC2021-WEPAB289

[3] M. Nabinger *et al.*, "Transverse and Longitudinal Modulation of Photoinjection Pulses at FLUTE," presented at IPAC'22, Bangkok, Thailand, Jun. 2022, paper TUPOPT068, this conference.

[4] M. Yan *et al.*, "Optimization of THz Radiation Pulses at FLUTE," in *Proc. of International Particle Accelerator Conference (IPAC'16), Busan, Korea, May 8-13, 2016*, Busan, Korea, 2016, pp. 3067–3069, doi:doi:10.18429/JACoW-IPAC2016-WEPOY037

[5] O. Kramer, *Genetic Algorithm Essentials*, 1st. Springer Publishing Company, Incorporated, 2017.

[6] J. Gonzalez *et al.*, "Batch bayesian optimization via local penalization," in *Proceedings of the 19th International Conference on Artificial Intelligence and Statistics*, vol. 51, 2016, pp. 648–657.

[7] D. R. Jones *et al.*, "Efficient Global Optimization of Expensive Black-Box Functions," *J. Glob. Optim.*, vol. 13, no. 4, pp. 455–492, 1998, doi:10.1023/A:1008306431147

[8] M. Schwarz *et al.*, "Analytic calculation of the electric field of a coherent THz pulse," *Phys. Rev. ST Accel. Beams*, vol. 17, p. 050 701, 5 2014, doi:10.1103/PhysRevSTAB.17.050701

[9] M. Schwarz *et al.*, "Analytic Calculation of Electric Fields of Coherent THz Pulses," in *Proc. IPAC'14*, Dresden, Germany, Jun. 2014, pp. 234–236, doi:10.18429/JACoW-IPAC2014-MOPRO067

[10] K. Flöttemann, *ASTRA: A Space Charge Tracking Algorithm*, https://www.desy.de/~mpyflo/

[11] I. Agapov *et al.*, "OCELOT: A software framework for synchrotron light source and FEL studies," *Nucl. Instrum. Meth. A*, vol. 768, pp. 151–156, 2014, doi:10.1016/j.nima.2014.09.057